Applied Water Science (2024) 14:39
https://doi.org/10.1007/s13201-023-02098-8

ORIGINAL ARTICLE

Synthesize of heterostructure TiO_2 by simultaneous doping of double silver and phosphate to degradation of methylene blue under visible light

Zohre Moeini[1,2] · Mohammad Hoseini[1] · Mansooreh Dehghani[1] · Mohammadreza Samaei[1] · Saeed Jafari[3] · Mahmoud Taghavi[4] · Abooalfazl Azhdarpoor[1]

Received: 19 October 2023 / Accepted: 25 December 2023 / Published online: 7 February 2024

Abstract

Photocatalysts show great potential as compounds for restoring contaminated water and wastewater resources. The study aims to synthesize a composite with high photocatalytic potential under visible light to photodegrade the organic pollutants. Ag/Ag_3PO_4@ TiO_2 were synthesized by doping Ag and Ag_3PO_4 on TiO_2. The composite was characterized using X-ray diffraction analysis (XRD), diffuse reflectance spectroscopy, Field emission scanning electron microscopy, and Energy-dispersive X-ray spectroscopy analyses, and its photodegradation ability was investigated by methylene blue. Utilization of pure TiO_2 yielded a removal efficiency that was merely half of the efficiency achieved when using modified particles, owing to the reduction of TiO_2 s band gap from 3.2 to 1.94 eV. In addition to its enhanced photocatalytic performance under visible light, the synthesized $Ag/Ag_3PO_4@TiO_2$ photocatalyst demonstrated remarkable efficiency in removing dyes such as methylene blue from aqueous solutions. The removal efficiency at pH less than 7 in 50 ppm methylene blue solution using 3 g/l photocatalyst over 45 min visible light irradiation was approximately 90 percent. Under sunlight, photocatalytic reactions exhibited an efficiency of over 95 percent within 45 min. It can be concluded that the simultaneous introduction of metallic (Ag) and nonmetallic (PO_4^{3-}) dopants significantly increases the efficiency of electron–hole recombination suppression in the photocatalyst and also decreases the band gap.

Keywords $Ag/Ag_3PO_4@TiO_2$ · Methylene blue · Photodegradation · Titanium dioxide · Visible light

✉ Abooalfazl Azhdarpoor
azhdarpoor@sums.ac.ir

Zohre Moeini
meini.zohre@yahoo.com

Mohammad Hoseini
hoseini2174@gmail.com

Mansooreh Dehghani
mandehghani@yahoo.com

Mohammadreza Samaei
mrsamaei@gmail.com

Saeed Jafari
jafari4514@yahoo.com

Mahmoud Taghavi
taghavi66@yahoo.com

[1] Department of Environmental Health, School of Health, Shiraz University of Medical Sciences, Shiraz, Iran

[2] Department of Environmental Health Engineering, School of Health, Student Research Committee, Shiraz University of Medical Sciences, Shiraz, Iran

[3] Department of Occupational Health and Safety Engineering, School of Health, Shiraz University of Medical Sciences, Shiraz, Iran

[4] Department of Environment Health Engineering, School of Health, Social Determinates of Health Research Center, Gonabad University of Medical Sciences, Gonabad, Iran

Introduction

Different organic dyes are used in various industries, such as cosmetics, textiles, paper, pharmaceuticals, and food. The wastewater from these industries contains a considerable quantity of toxic and carcinogen dyes (Alver et al. 2020). Methylene blue (MB) is a cationic widely used dye in industries that can cause adverse health effects such as tachycardia, vomiting and nausea, neuronal apoptosis, extreme sweating, leptomeninges, eye irritation, and mental disorders (Alver et al. 2020; Moztahida and Lee 2020; Wang et al. 2014).

Different methods like chemical, photochemical, physical, biological, and electrochemical are employed for the degradation of chemical pollutants and their removal from the ecosystem (Otari and Yadav 2019). Photocatalytic methods are applied to degrade organic matter due to their positive aspects such as the application of inexpensive and non-hazardous catalysts, low power requirements, and mild chemicals (Karanasios et al. 2015). Sunlight is the most available and renewable energy source that can be utilized as the activation energy in photocatalytic processes (Otari and Yadav 2019).

Various semiconductors have been used to photodegrade organic matter (e.g., ZnO, SnO_2, WO_3, and TiO_2). Among the various semiconductors, titanium dioxide (TiO_2) is the most convenient since its chemical stability, low cost, and high efficiency (Sun et al. 2020). Semiconductors have the potential to produce pairs of electrons and holes when exposed to light. It occurs when the electrons are elevated from the valence band (VB) to the conducting band (CB), resulting in an electron–hole pair. The photogenerated electron then moves to the surface of the semiconductor where it can undergo a redox reduction reaction (Mosavi et al. 2021). The main defect of TiO_2 is its relatively high band gap (3.2 electron volt (eV)). By the high band gap, it absorbs only photon energy in the area of the ultraviolet (UV) light. UV radiation accounts for only 3% of sunlight, so the photoelectrochemical properties of the single-component semiconductor should be modified to consume more solar energy (Dette et al. 2014). It is approved that the doping metallic or nonmetallic elements reduce the band gap and shift the adsorption edge to the visible spectrum range. The purpose of doping some elements is to lower the conduction band and decrease the band gap energy (Schneider et al. 2014). Creating a hybrid between silver elements and semiconductors is an approach to designing silver composites. Creating a hybrid between silver and semiconducting structures is an approach to designing silver compound composites. This process leads to optical properties due to the conductivity of the hybrid metal–semiconductor structure and an increase in charge transfer (Cushing et al. 2012; Mosavi et al. 2021; Singh et al. 2019; Yang et al. 2013). Species of silver, owing to the surface plasmonic resonance effect, can absorb visible light-considerably. Moreover, since Ag_3PO_4 is a visible light driven semiconductor, doping Ag^o element inhibits the reductive degradation of Ag_3PO_4. Hence, combining silver as an electron acceptor and silver phosphate as a visible-light-driven semiconductor in Ag/Ag_3PO_4 particles with TiO_2 increases its adsorption, charge separation, and transfer between the surface and interface for photo-generated carriers. This modification enhances the effectiveness of silver by absorbing light, stimulating the semiconductor, and added advantage of heightened stability to the composite in double heterostructure of $Ag/Ag_3PO_4@TiO_2$ (Teng et al. 2013; Zhou et al. 2015).

The modification process of titanium dioxide reduces the band gap energy, and improves the photocatalytic properties, and also introduces antibacterial properties by adding silver (Ahmad Barudin et al. 2013). This enhancement presents the dual heterostructure as an attractive option for various improvements in photocatalytic applications.

The study focuses on enhancing of the photocatalytic properties of titanium dioxide (TiO_2) by creating a dual heterostructure with silver. This modification aims to address the limitation of TiO_2's relatively high band gap, which absorbs only UV light, by introducing silver (metallic dopant) as an electron acceptor and silver phosphate (non-metallic dopant) as a visible light-driven semiconductor. The particle, synthesized in powder form, is employed without any additional substrate or media for the photocatalytic removal of methylene blue. In the current study, $Ag/Ag_3PO_4@TiO_2$ heterostructure composites are synthesized and characterized by morphological, electrochemical, and elemental analyses. MB was studied as the target pollutant to assess the synthesized composite's efficiency in removing organic dyes. The removal efficiency of modified particles in the MB removal was compared with the efficiency of titanium dioxide under visible and ultraviolet light irradiation. In addition, the influence of several effective parameters, such as initial pollutant concentration, pH, contact time, and photocatalyst dose on efficacy was investigated to reach the optimum condition.

Materials and methods

Materials

The chemicals used were analytical and synthesized grade. They were used without further purifying. Methylene Blue (MB) dye, silver nitrate ($AgNO_3$, 99%), Monosodium phosphate (NaH_2PO_4, 99%), Titanium dioxide powder

Table 1 Table of the abbreviations, their extended form, and root of word

Abbreviation	Expansions
XRD	X-Ray diffraction analysis
DRS	Diffuse reflectance spectroscopy
FESEM	Field emission scanning electron microscopy
EDS	Energy-dispersive X-ray spectroscopy
MB	Methylene Blue
Ag	Silver
TiO_2	Titanium dioxide
VB	Valence band
eV	Electron volt
UV	Ultraviolet

(Degussa P-25, TiO_2), and Ethanol were purchased from Merck Co, Germany. Deionized water was used in all steps of experiments.

Synthesis of Ag @TiO_2

First, 1 g of TiO_2 powder was dissolved into 50 ml deionized water. Then, 0.05g of $AgNO_3$ was added to the solution on the stirrer. It was stirred for 30 min at 70 °C. The resulting sediments were calcinated for 3h at 400 °C.

Synthesis of Ag/Ag_3PO_4@TiO_2

In the second step, 2g of NaH_2PO_4 was dissolved in 40 ml of water. Then, 0.5 g of powder obtained in the preceding step was added to the solution (solution A).

After that, 0.5 g $AgNO_3$ was dissolved in 30 ml of distilled water (solution B). After this, solution B was added to solution A on the stirrer. Yellowish precipitation was collected and washed with distilled water a few times. The final sediments were dried at 80 °C over the night.

Characterization of the photocatalyst

X-ray diffraction (XRD) is used to discover the nature of materials as either crystalline or amorphous (Table 1). The advanced D8 X-ray diffractometer from Bruker Company was used to study the crystal structure. The X-ray source used was a monochromatic (Ka Cu) radiation source with a wavelength of 0.15418 nm at 40 kV and 40 mA. Particles of photocatalyst were scanned in the range of position 10 to 80.

The microstructure and morphology of the samples were studied using field-transmitted electron microscopy (FE-SEM, TESCAN MIRA3) with an acceleration voltage of 20.0 kV. The elemental analysis and concentrations of dopants were verified using Energy-Dispersive X-ray (EDS) analysis. UV Diffuse Reflectance Spectroscopy (DRS) (S_4100, SCINCO Co.) was used to determine the band gap energy of particles and light absorption properties. The range of the wavelength for the Spectrophotometer was 300 to 1000 nm. Fourier-transform infrared (FTIR) spectroscopy is used to analyze the molecular composition of synthesized photocatalyst. An ABB Bomen MB 100 Spectrometer (Thermo, AVATAR, U.S.A) was used to record the Fourier transform infrared (FTIR) spectra from 400 to 4000 cm^{-1}.

Photocatalysis experiment

The photocatalytic activity of the Ag/Ag_3PO_4@TiO_2 particles in MB degradation was examined in a photoreactor under a Xenon lamp (100 W). The batch reactor was a 100 ml Pyrex container. All experiments were carried out using distilled water and at ambient temperature. Solutions were prepared of a 2000 ppm stock of MB daily. Some influential factors, including the initial concentration of pollutant (25–100 ppm), photocatalyst dose (0.4–4 g/l), pH (3–11), and time (5–120 min), were investigated and optimized. All experiments were repeated twice.

To compare the efficiency of the synthesized particle with the essential titanium dioxide, all the experiments were repeated using TiO_2-P25 powder under 30 W ultraviolet light and 100 W xenon visible light under the same conditions. At last, employing entirely analogous conditions, the efficacy of the photocatalyst was surveyed in the presence of sunlight.

The desired pH was adjusted using 0.1 N hydrochloric acid and sodium hydroxide. Each sample was agitated in the dark for 30 min before illumination to achieve an equilibrium of adsorption–desorption. The solution was then irradiated with visible light from the top of the container. The photocatalyst was removed from the solution through a centrifuge. Subsequently, the residual concentration of MB was determined by UV–vis spectrophotometry (Hach, DR5000) at 663 nm.

The removal efficiency was calculated using Eq. (1).

$$R\ (\%) = \left(C_0 - C_e\right)/C_0 \tag{1}$$

Photocatalytic kinetic models

The kinetics of photocatalytic reactions was investigating using first-order model and Langmuir–Hinshelwood (L–H) rate equation based on the Levenberg–Marquardt algorithm. The degradation of organic pollutants was examined using these models in the optimal experimental conditions studied (Dewidar et al. 2018; Khezami et al. 2016). The kinetic model at first order provided valuable insights about the degradation kinetics of the targeted compounds (Eq. 2) (Li et al. 2008).

Application of this model is as the following expression (Eq. 3) (Alkaykh et al. 2020):

$$\ln\left(\frac{C_t}{C_0}\right) = -\mathrm{Kt} \tag{2}$$

The investigation of photocatalysis kinetics was conducted by agitating a 50-mL solution of MB with an initial concentration (C_0) of 50 mg/l dye with 2 g/l of prepared photocatalyst (pH = 7). The concentration at specific times intervals (C_t) was measured.

The L–H equation is commonly employed to explain the dynamics of surface-catalyzed reactions, especially when dealing with heterogeneous catalysis. By analyzing the equilibrium constants for reactant adsorption on the catalyst surface and the rate constant for the surface reaction, the L–H rate expression for a given reaction can be determined. To examine the behavior of weakly adsorbed products with low coverage on the catalyst surface and no significant reverse reaction, the L–H model is highly useful. The L–H equation can help analyze and optimize catalytic processes by providing valuable insights into the reaction mechanism at the catalyst surface (Lin et al. 2015).

$$r = -\frac{\mathrm{d}C}{\mathrm{d}t} = \frac{k_r K_e C}{1 + K_e C} \tag{3}$$

the parameters of the equation are as follows:

r is reaction rate, C presents the concentration of solution (mg/l), and k_r and K_e are reaction and equilibrium constant, respectively (Asenjo et al. 2013).

Results and discussion

Characterization of $Ag/Ag_3PO_4@TiO_2$

The XRD pattern obtained from $Ag/Ag_3PO_4@$ TiO_2 and pure TiO_2 is demonstrated in Fig. 1. It complied with the pattern in previous research (Peng et al. 2019). It showed that a stable heterojunction structure was successfully formed from Ag_3PO_4 and anatase TiO_2. The diffraction analysis in

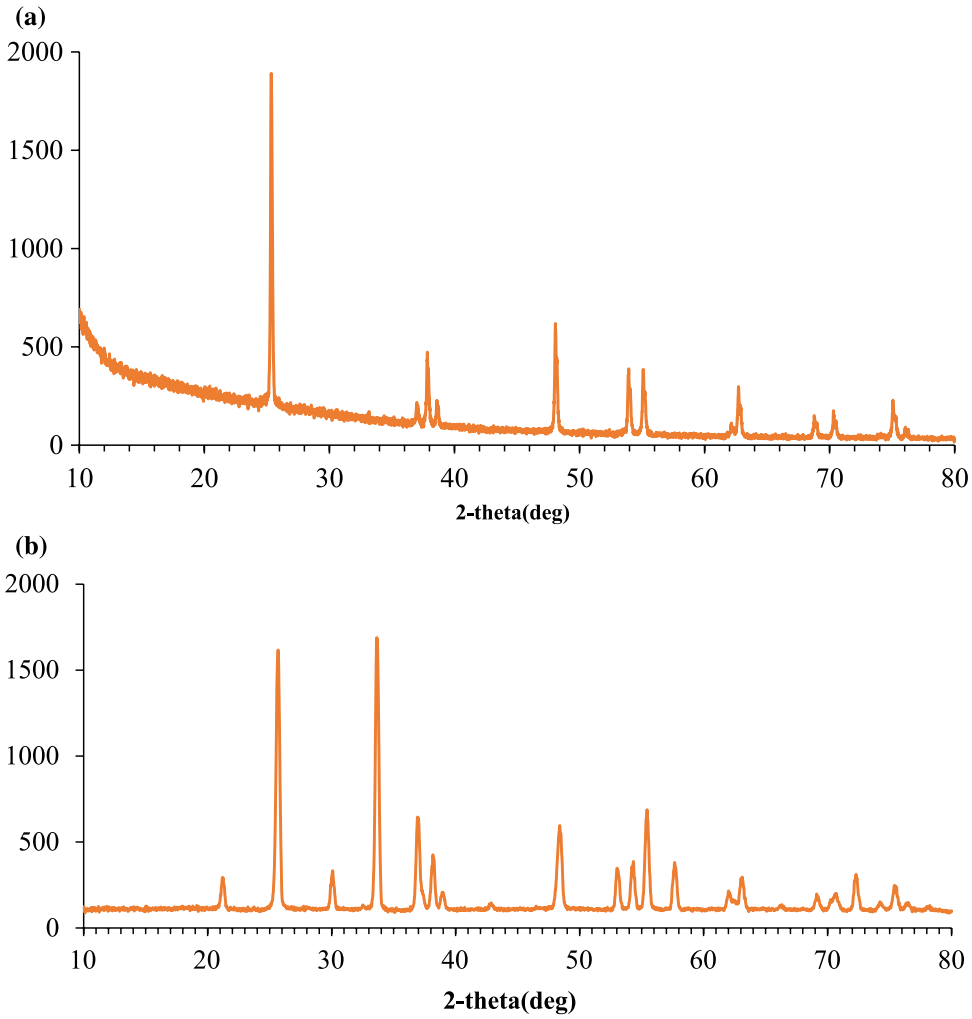

Fig. 1 XRD pattern for **a** Pure TiO_2 P25 **b** $Ag/Ag_3PO_4@TiO_2$

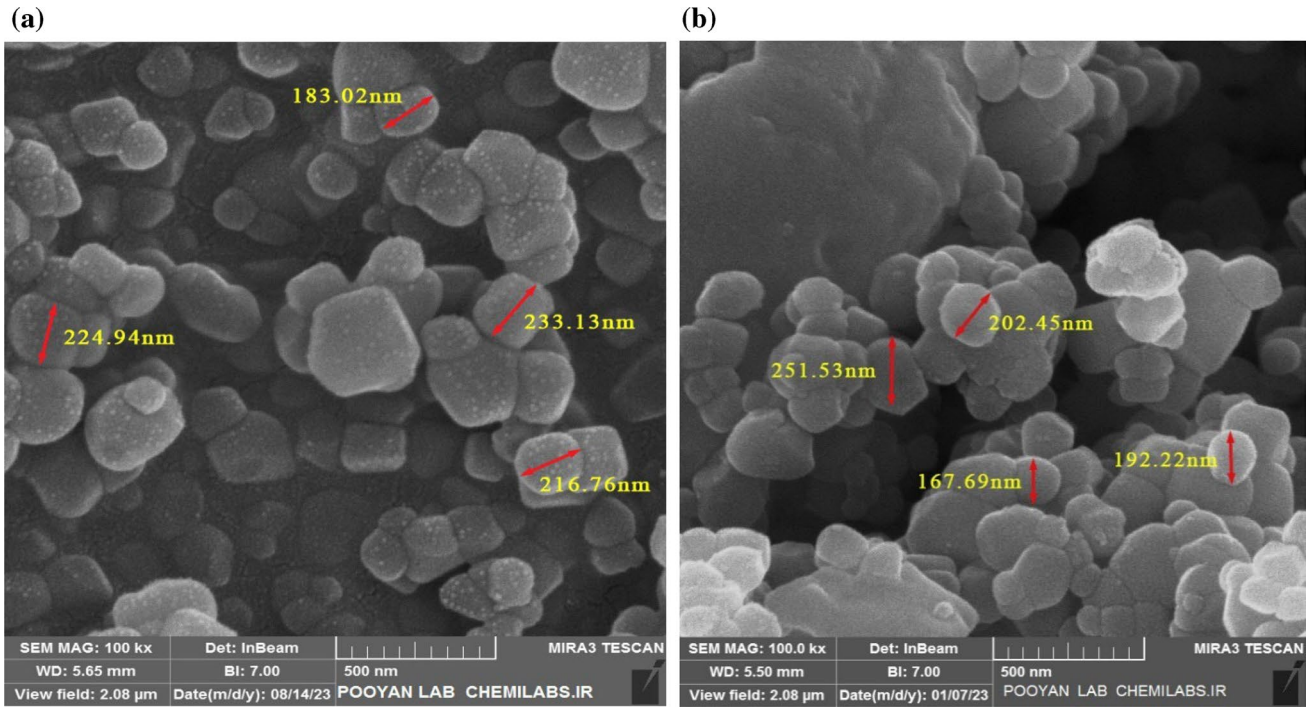

Fig. 2 FESEM images of **a** Pure TiO_2 P25 **b** $Ag/Ag_3PO_4@TiO_2$ at 500kx magnification

Fig. 1a shows that the diffraction peaks observed at Bragg angles (2θ) of 25.8, 38.2, 48.3, 55.2, 57.8, 63, 72.2 and 75.3° correspond to the lattice planes of anatase TiO_2. Doping elements have led to the emergence of multiple peaks except for the peaks. In Fig. 1b, sharp peaks of diffraction were appeared at 2θ value of 21.12, 25.8, 30.1, 33.8, 37, 38.2, 48.3, 53, 55.2, 57.8, 63, 72.2, 74.1, and 75.3°. These peaks were found in the study of Teng et al. (Teng et al. 2013). Findings indicate that Ag/Ag_3PO_4 particles were deposited onto the surface of the TiO_2.

FESEM and the resulting images examined the morphology of the synthesized composite and pure TiO_2, shown in Fig. 2. Images are obtained at 500 k magnification. As illustrated in Fig. 2a, the particle size of TiO_2 was 181–233 nm (mean particle size, 214 nm), and the size of composites was 167–251 (mean particle size, 204 nm). Moreover, a comparison between the current images and the existing FESEM images proved that the composite is compatible with other studies regarding geometric and surface morphology. It highlighted the correct formation of heterostructure particles during the synthesis process. (Nyankson et al. 2021). The

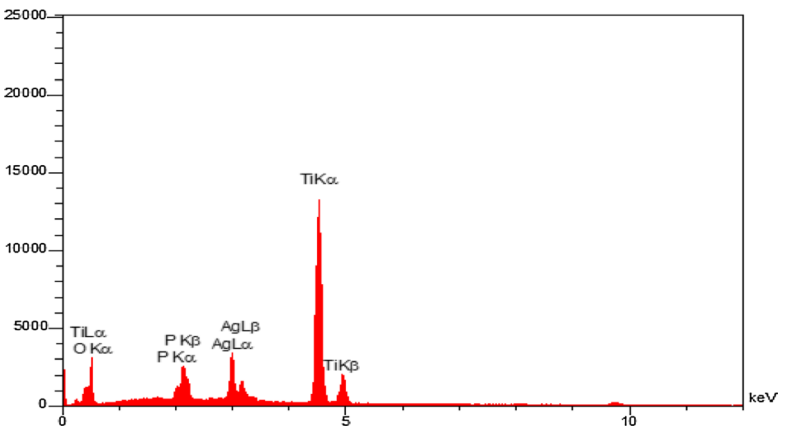

Fig. 3 EDX spectrum of $Ag/Ag_3PO_4@TiO_2$

O	Ag	P	Ti
31.49	11.92	3.28	53.30

study did not observe any noteworthy changes in the dimensions of TiO_2 particles (Liu et al. 2019; Peng et al. 2017).

As shown in the figures, the geometric shape of particles is a rounded cubic. A high level of arrangement and layout in high and low magnification FESEM images indicates that TiO_2 nanoparticles (NPs) are modified without losing their architectural structure after the deposition of Ag/Ag_3PO_4. The rough surface of the particles states that some other tiny NPs have adhered to the surface of TiO_2. This phenomenon causes TiO_2 porous anatase to provide very beneficial sites for adsorbing positively charged silver ions (Ag^+), which will limit the growth of Ag_3PO_4 particulates (Nyankson et al. 2021; Peng et al. 2019).

The chemical composition of $Ag/Ag_3PO_4@TiO_2$ is depicted in Fig. 3. It proved the presence of oxygen (O), silver (Ag), phosphorus (P), and titanium (Ti) in amounts of 31.49, 11.92, 3.28, and 53.30 W%, respectively. Furthermore, chemical analysis revealed that doping elements are doped on the titanium oxide particles.

The UV–Vis diffused reflectance spectra of the $Ag/Ag_3PO_4@TiO_2$ particles are shown in Fig. 4. The band gap was calculated from UV–Vis absorption spectra using Tauc Plot method using Fig. 4b. The estimated band gap of the synthesized particles in the current study was approximately 1.94 eV. The comparison between the band gap of the pure TiO_2 (3.2 eV) and pure Ag_3PO_4 (2.4 eV) showed that it is decreased to 1.94 eV in $Ag/Ag_3PO_4@TiO_2$ by doping Ag and Ag_3PO_4 on the TiO_2 as dopants (Del Angel et al. 2018; Farooq et al. 2019; Nagaraj et al. 2019). Also, Liu et al., showed that the obvious absorption range and band gap energy of pure Ag_3PO_4 were 450 to 500 nm and 2.45 eV, respectively (Liu et al. 2019). A significant change toward red implies the use of visible light energy. The findings showed a high absorption within the visible light range. Its absorption edge was about 638 nm. This is in line with other outcomes. Improved light absorption properties can lead to improved photocatalytic efficiency of particles. Furthermore, it can be concluded that the doping agents (Ag and Ag_3PO_4) are doped on the P-25 successfully. In the study by Teng et al., the shape of the absorption peak of the $Ag/Ag_3PO_4/TiO_2$ nanotubes was the most similar to the peak of the Ag/TiO_2 nanotubes. They asserted that an absorption peak of about 450 nm can be due to the surface plasmon resonance of silver NPs in $Ag/Ag_3PO_4/TiO_2$ (Teng et al. 2013).

In Fig. 5, the FTIR spectra of $Ag/Ag_3PO_4@TiO_2$ show distinctive absorption bands that are associated with the

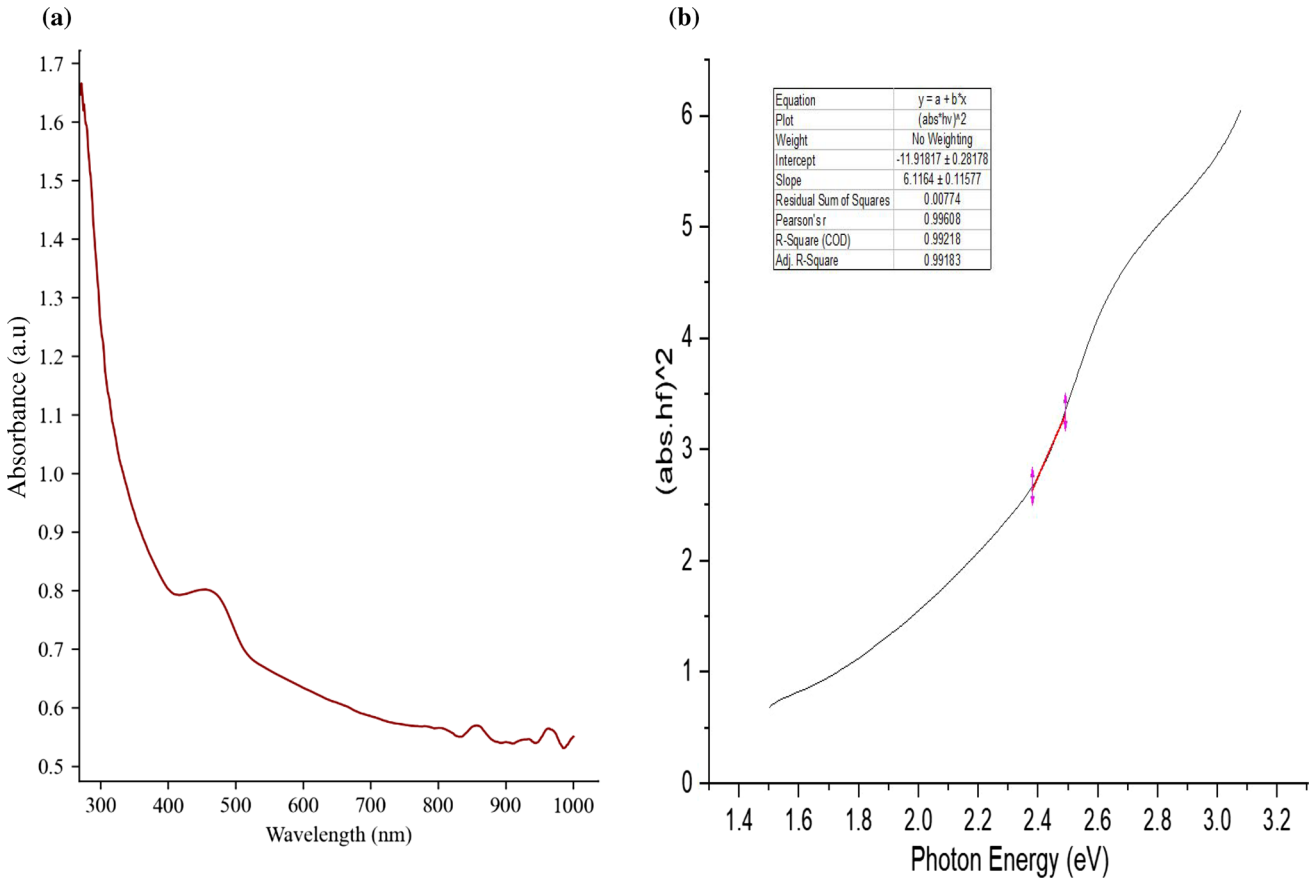

Fig. 4 **a** DRS spectra of $Ag/Ag_3PO_4@TiO_2$ by Absorbance–wavelength **b** Tauc's plot of $Ag/Ag_3PO_4@TiO_2$

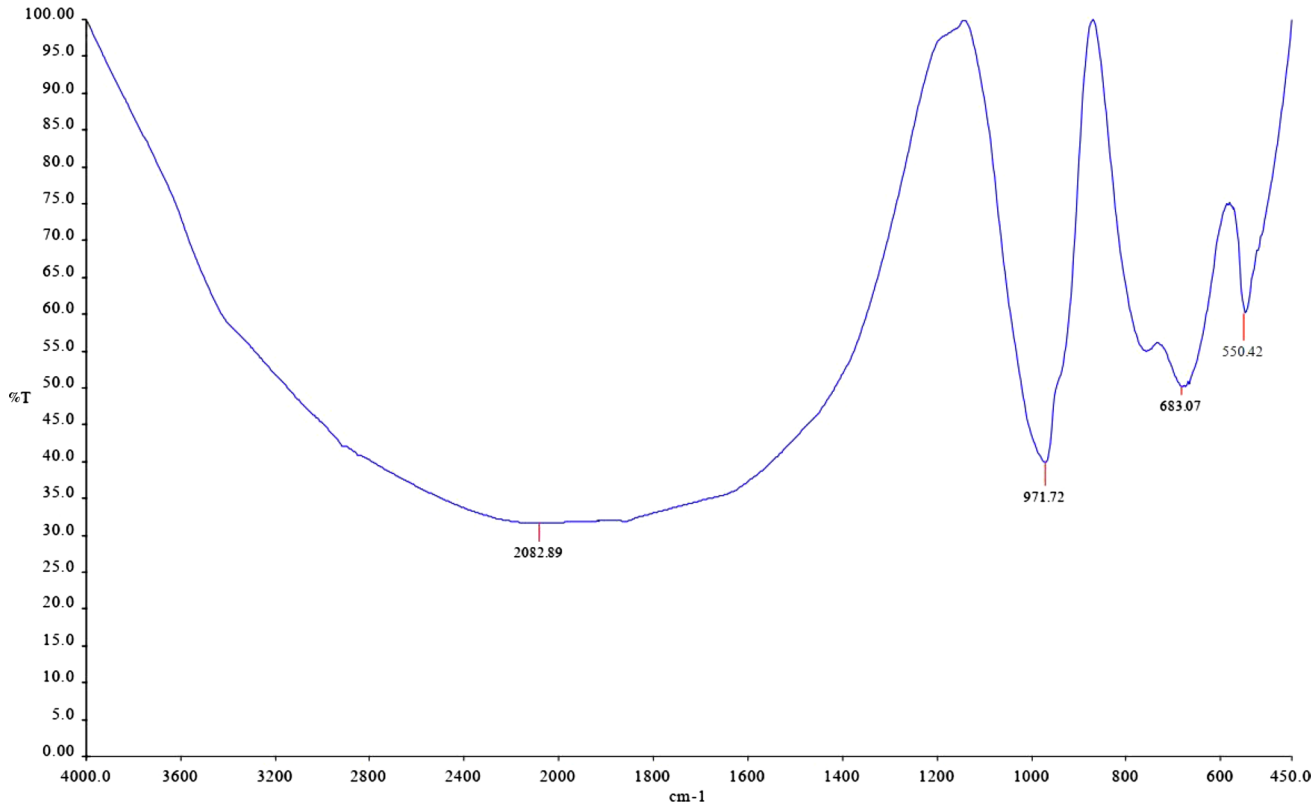

Fig. 5 The FTIR spectra of $Ag/Ag_3PO_4@TiO_2$

molecular vibrations of the individual components, such as TiO_2, Ag, and Ag_3PO_4. The chemical composition and bonding environments of the photocatalyst can be characterized and its properties can be understood with the help of these distinctive absorption bands. The detected peak at 550 cm^{-1} corresponds to the vibration of the O=PO group (H. Liu et al. 2019). The Ti–O bond's stretching vibration peak is observed at 683 cm^{-1} (Ding et al. 2019; Hu et al. 2021). The strong and narrow band at 971 cm^{-1} is due to the stretching vibration corresponds to P–O band (Liu et al. 2019). The stretching and bending vibrations of hydroxyl groups (OH) on the surface of TiO_2 caused an intense and wide absorption peak at 2082 cm^{-1}, which was noted. The wide peak within the 2000–3000 cm^{-1}

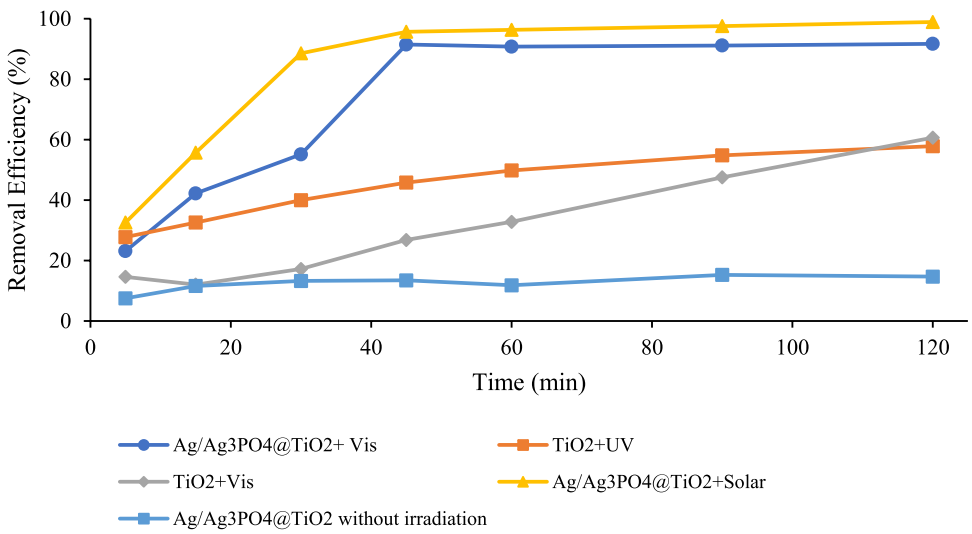

Fig. 6 The effect of time on MB removal efficiency using $Ag/Ag3PO4@TiO_2$ and TiO_2 (pH 7, concentration 50 mg/l, adsorbent dosage 2 g/l)

range may result from the absorption of water (Song and He 2017).

The effect of time on MB removal

The duration of the contact between the photocatalyst and pollutant under irradiation affects the removal efficiency. To investigate the effect of irradiation time, the pH, initial concentration of MB, and dose of photocatalyst were 7, 50 ppm, and 2 g/l, respectively. Photodegradation of MB was evaluated at time intervals of 0–120 min (5, 15, 30, 45, 60, 90, and 120 min), and the results are presented in Fig. 6. For the sake of comparison, results obtained using the commercial TiO_2 P25 under UV and visible light are also reported. Moreover, Fig. 6 illustrates the outcomes of methylene blue removal without of light, providing insights into surface adsorption levels. This distinction aids in discerning between photocatalytic removal efficiency and adsorption processes. The adsorption process achieved the highest removal efficiency at around 15 percent within 90 min. Hence, the adsorption process itself played a minor role in removing MB. Based on the results, it can be concluded that the primary factor for removal was optical degradation.

The results demonstrated that MB is removed more than 90 percent after 45 min using $Ag/Ag_3PO_4@TiO_2$. At the same time, using P-25 under visible and ultraviolet light, 26.80 and 45.78% of MB have been removed. The outcomes derived from the investigation of solar energy's impact on the photocatalytic process revealed that a remarkable 88.5% of methylene blue was successfully removed within 30 min.

No further removal occurred after 45 min. More vacant and active sites on composites may be the reason for the high rate of absorption and photodegradation of MB over the first 45 min. In the study of Ashrafi et al., 78% of MB was removed in 30 min. They claimed that the time of irradiation and contact between the pollutant and photocatalyst is the most important factor in the removal. The dominant mechanism of removal in the 30 and 45min was adsorption and photocatalysis, respectively (Nyankson et al. 2021). In contrast to our study, study Abukhadra et al. identified the initial 5 min of radiation as the optimal time (Abukhadra et al. 2018). The disparity in optimal times could be attributed to variations in target pollutants and a lower initial concentration in that particular study. As MB is photodegraded during irradiation time, the competition between producing intermediates and MB molecules for absorbing to photocatalysts is intense (Xu et al. 2014). Additionally, intermediate and by-product compounds may compete with MB molecules for oxidation by active species (Khan et al. 2022). Regarding the result of the current study, 45 min can be the most cost-effective time for the photodegradation of MB using $Ag/Ag_3PO_4@TiO_2$. Generally, the effect of time on the removal of methylene blue through photocatalysis is a critical aspect that significantly impacts the efficiency of the process. Optimizing irradiation time can effectively enhance the photocatalytic removal of methylene blue, thereby contributing developing more effective water treatment technologies.

The study conducted by Rupa et al. is in line with our present investigation. Their research they examined the effectiveness of removing reactive Yellow-17 within 60 min using modified titanium dioxide with Ag and pure P-25. The results showed a removal efficiency of 77 and 22% under visible light and 64 and 34% under UV light for Ag-modified and pure P-25, respectively. The electronic interaction at the interface between the metal deposits and the semiconductor surface can explain the boosted performance of Ag. This interaction causes the transfer of electrons from TiO_2 to the surrounding area of the metal particle, leading to the

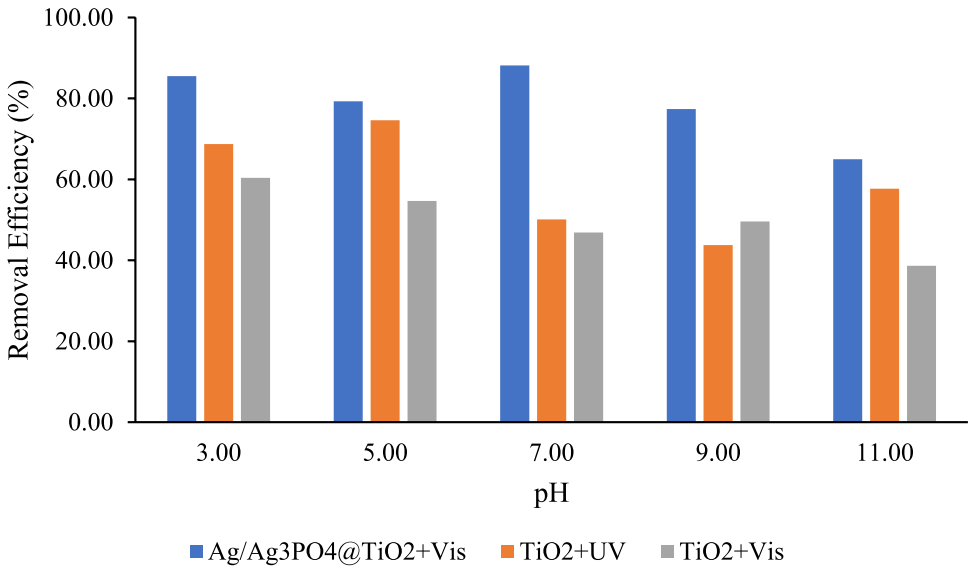

Fig. 7 The effect of pH on MB removal efficiency using $Ag/Ag_3PO_4@TiO_2$ and TiO_2 (concentration 50 mg/l, adsorbent dosage 2 g/l, time 45 min)

creation of Schottky barriers. As a result, charge separation occurs, contributing to the enhanced activity observed (Rupa et al. 2007).

The effect of pH on MB removal

The pH is a crucial role in removal procedures due to changes in surface physicochemical properties of pollutants or photocatalysts. The impact of pH on the photodegradation and adsorption of MB by 2 g/l of $Ag/Ag_3PO_4@TiO_2$ and P-25 was investigated at 45 min with an initial concentration of 50 ppm in the pH range of 3–11 (Fig. 7). The findings indicated that the efficiency at pH 3 to 7 does not show considerable changes. The efficacy of pH 7 was 88.15 percent using $Ag/Ag_3PO_4@TiO_2$ and 46.88 using TiO_2, respectively. Generally, pH 7 and below are most effective in removing of MB. Around pH 7–8, the hydroxyl ions present are readily converted into hydroxyl radicals, which, in a cascading effect, might be accountable for breaking down the dye molecules (Rupa et al. 2007). Some important mechanisms in the removal process include oxidation by H+, attack by hydroxyl radical, and reduction by conducting band negatively charged electrons (e-) depending on pH, hydroxyl (OH–), and hydron (H+) ions (Alkaim et al. 2014). Nevertheless, when the pH values are high, the degradation efficiency decreases because of the electrostatic repulsion between the anionic dye surface and the hydroxyl anions. As a result, they are unable to interact effectively with the dye molecules (Rupa et al. 2007). The results from the Moztahida and Lee study were contrary to ours. They expressed that the adsorption of MB was decreased at low pH = 3 because of competition with MB and excess hydrogen ions. Moreover, photoconversion was increased at high pH = 11 because of the strong attraction of MB molecules and the hydroxide ions (Moztahida and Lee 2020).

The pH of the dispersions significantly influences the reaction occurring on the semiconductor particle surface due to the amphoteric nature of most semiconductor oxides. The pH parameter directly affects the surface charge characteristics of the photocatalyst. Conversely, since the anionic dye molecule carries a negative charge, lower pH levels promote its adsorption on the catalyst surface (Alkaim et al. 2014). The positive surface charge of the MB enhances its adsorption to the composites of current photocatalyst with a negative surface charge (Nguyen and Kim 2022; Teng et al. 2013). Therefore, hydron and MB molecules are expected to compete for adsorption to the photocatalyst in an acidic medium. Surprisingly, in the acidic range, the removal of MB is improved. It can show that photodegradation is the dominant mechanism of MB removal. Photoconversion is intensified due to the presence of H+ in high quantities (Khan et al. 2022).

The effect of initial concentration of MB

The nature and initial concentration of the pollutant can influence the rate of its adsorption and photodegradation. The effect of different initial concentrations on the performance of $Ag/Ag_3PO_4@TiO_2$ and pure TiO_2 was examined under a similar situation (pH = 7, dosage of photocatalyst = 2 g/l, time = 30 and 45 min), and its results are depicted in Fig. 8.

Modified titanium dioxide showed higher efficiency at 30 min and 45 min at 25 ppm (68.88, 78.13 percent) and 50 ppm (57.29, 79.69 percent) rather than pure TiO_2 under visible and even UV irradiation. With a higher initial pollutant concentration, pure titanium dioxide's removal efficiency

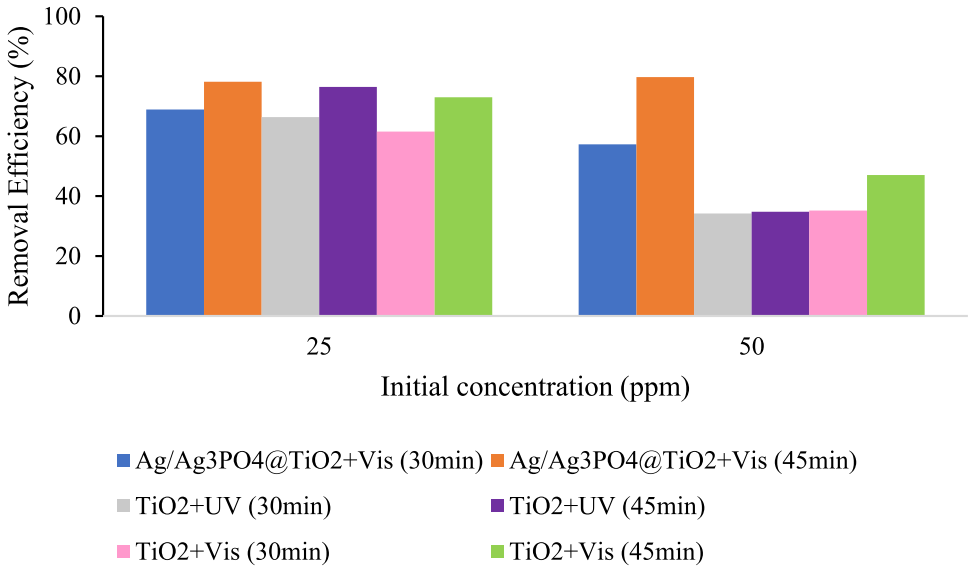

Fig. 8 The effect of initial concentration of MB using $Ag/Ag_3PO_4@TiO_2$ and TiO2 (pH = 7, dosage of photocatalyst = 2 g/l, time = 30 and 45 min)

decreases but increases with the photocatalyst. The difference is due to the distinct removal mechanisms used by these two materials. Adsorption is the primary method for removing pollutants with pure titanium dioxide, and photocatalysis is the primary mechanism in the case of modified titanium.

Besides, the low efficiency of MB decomposition by TiO_2, even under UV light at high concentration levels, may be due to the dark color of the solution and reduced absorption of light photons. Due to the wide band gap of pure TiO_2, a substantial number of high-energy photons are required for the photoexcitation of the photocatalyst. The dark color of the solution can function as a light filter, impeding the penetration of photons to the surface of the pure TiO_2. As the photodegradation of MB progresses, the solution undergoes a gradual lightening in color, indicative of an enhancement in the photocatalytic process (Gan et al. 2016).

In addition, active sites and empty pores are occupied at a high concentration, which can reduce the adsorption and photocatalyst rate. (Chanu et al. 2019). Less possibility of contact between MB molecules and photocatalyst particles in a solution with low initial concentration can lead to less removal. In a study by Pandey et al., they found that collisions and reactions between MB molecules and hydroxyl radicals decreased at a concentration beyond 3.00×10^{-6} M. They also stated that an increase in collisions between dye molecules could reduce the possibility of contact between pollutants and photocatalyst particles (Pandey et al. 2015). The study by Zheng et al. had different results than the current one. Their study revealed that increasing the initial methylene blue concentration resulted in a decrease in photocatalytic process efficiency. The differences in the photocatalytic strength of the catalyst particles and the range of studied initial concentrations could account for the variations in the results of the two studies. The photocatalyst's capacity to decompose methylene blue may decline if higher concentrations are explored in this study. Pollutant adsorption on the photocatalyst surface can lead to a decrease in efficiency, as photons are not able to be absorbed by the surface (Zhang et al. 2020).

The effect of the photocatalyst dose on MB removal

The effect of photocatalyst dose on MB removal was surveyed in different amounts of photocatalyst (0.4, 1, 2, 3, and 4), and its results are presented in Fig. 9. The performance results of the synthesized particle were compared with the performance efficiency of basic titanium oxide powder under visible and ultraviolet light irradiation. These tests were conducted at pH = 7, at 30 and 45 min, and an initial concentration of 50 ppm. Photodecomposition of MB increased from 23.14 to 86 percent with an increase in $Ag/Ag_3PO_4@TiO_2$ dose from 0 5 to 4 g/l over 45 min. The efficiency is ascending to 3 g/l and then descending with a gentle slope. The most removal, 93.44 percent, was accrued using 3 g/l of $Ag/Ag_3PO_4@TiO_2$. Increasing the composition dose causes an increase in active sites and the amount of O^{2-} and hydroxyl radicals (Jain and Shrivastava 2008). Anantha et al. have also shown that the degradation rate increases with increasing doses of photocatalyst to 20 mg. The removal efficiency of 60 mg/100 ml adsorbent particles. in MB solution with an initial concentration of 40 ppm at 45 min was 93.08 percent. They reported 2 mg/l as the optimum photocatalyst dosage. They expressed that exceeding the quantity of photocatalysts can cause scattering of light and aggregation of NPs (Anantha et al. 2020). Salehi et al. also indicated that photocatalysts with a higher amount than the optimal dose can be agglomerated and reduce their performance (Salehi et al. 2012).

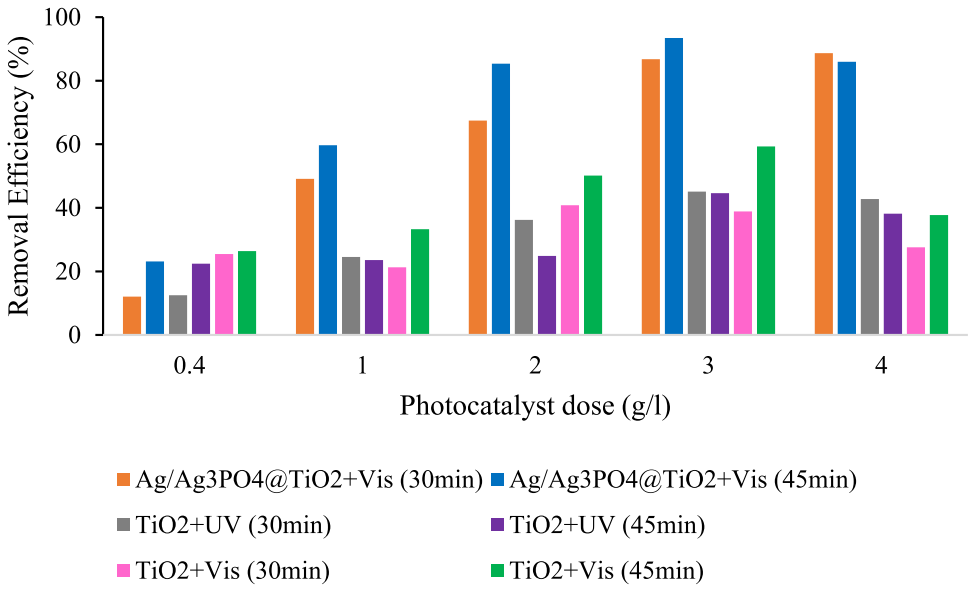

Fig. 9 The effect of $Ag/Ag_3PO_4@TiO_2$ and TiO_2 dose on the MB removal (pH = 7, concentration 50 ppm, time 30 and 45 min)

The removal efficiency of MB with 4 g/l of pure titanium dioxide under visible and UV light was 37.71 and 38.18 percent, respectively. The disparity in removal efficiency of titanium dioxide under visible and ultraviolet light is negligible. Thus, it can be inferred that the removal of MB was most likely due to adsorption rather than undergoing photodegradation. Given the band gap of titanium dioxide being 3.2 eV, it is probable that the power and intensity of the utilized ultraviolet light are insufficient to cover this band gap (Alamu et al. 2021). The findings validate the decrease in titanium dioxide's bandgap via doping silver and phosphate doping. A comparison of

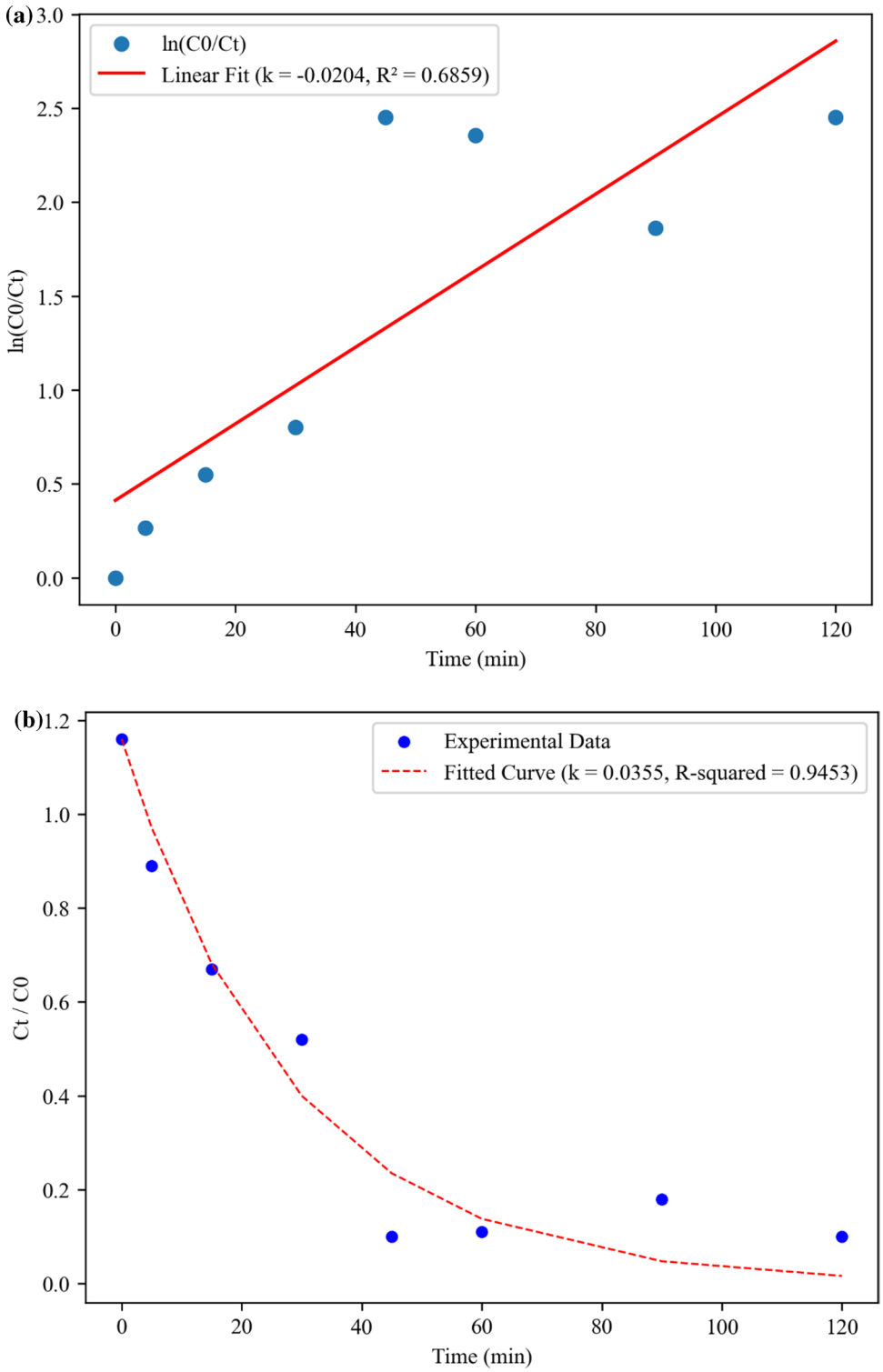

Fig. 10 Plot of **a** first-order kinetics of MB degradation on $Ag/Ag_3PO_4@TiO_2$ **b** Langmuir–Hinshelwood kinetics model

removal rates using synthesized structures under visible light and pure TiO_2 under UV light shows that the studied photocatalyst effectively degrades the pollutants in the visible light spectrum. Doping metal and non-metal elements can reduce the bandgap of the TiO_2. Because the valence band level of Ag_3PO_4 is lower than that of TiO_2, the sensitization of Ag_3PO_4 to visible light prompts the transfer of holes from Ag_3PO_4 to TiO_2. Consequently, the holes formed in the valence band of TiO_2 can effectively trigger the decomposition of MB (Rawal et al. 2012).

Kinetics of photocatalytic degradation

To investigate kinetic degradation of MB, two first-order and Langmuir Hinshelwood (L–H) models are employed (Fig. 10a, and b). It is evident that the L–H model has a higher R-squared value of 0.94, which is higher than the first-order model's R-squared value of 0.68. The L–H model is an advanced model that compares to the first-order model and considers the adsorption of the pollutant on the photocatalyst surface. The L–H model is likely to provide a more accurate fit to the data due to its more realistic representation of the photocatalytic process. Compared to the rate constant of − 0.0204 for the first-order model, the L–H model's rate constant is higher at 0.0355. The L–H model is predicted to have a faster reaction rate, which is consistent with the more realistic depiction of the photocatalytic process, based on the information provided. The L–H model has been proven to be more accurate for the photocatalytic kinetic data than the first-order model, according to the above results. Asenjo et al. investigated the use of L–H and first-order equations to demonstrate the absence of synergy effect in photocatalytic degradation of phenol. They asserted that although first-order kinetics can simplify calculations, depending solely on this approach can lead to inaccurate conclusions if the actual kinetic pattern differs from first-order behavior (Asenjo et al. 2013).

The mechanisms of photocatalytic activity of Ag_3PO_4/TiO_2 composite

The light properties showed that doping organic and inorganic material enhanced the photocatalytic activity of the heterostructure composite rather than pure TiO_2. The improvement can be due to an efficient charge separation and subsequent decline of electron–hole recombination. This is due to the alignment of the bands between TiO_2 and Ag_3PO_4 in heterostructure particles. This unparalleled band matching results in higher photocatalytic activity of the coupled semiconductor to the bare TiO_2 and Ag_3PO_4 (Samal et al. 2018; Xu et al. 2021). Modification of TiO_2 makes separating the electron from the hole. Additionally, inhibition of recombination photogenerated electrons and holes (electron–hole recombination) can improve the photocatalytic activity (Hamrouni et al. 2020). In this process, Ag_3PO_4 is a sensitizer to absorb visible light, and TiO_2 acts as a substrate. When heterostructure particles are exposed to light, the holes generated by the photons are rapidly transferred from the Valence Band (VB) Ag_3PO_4 to TiO_2 rapidly due to the established electrical field. As a consequence, the recombination of the electron and the hole is hindered (Liu et al. 2019; Tang et al. 2014).

While the adsorbed dyes can provide a small boost in TiO_2's photocatalytic performance under visible light, the substantial enhancement seen in Ag_3PO_4/TiO_2 is mainly attributed to the added Ag_3PO_4 particles, which play a crucial role in promoting the photocatalytic efficiency of the composite material (Yao et al. 2012). Photonic energy excites the composites by irradiation of visible light. An excited electron from the valence band is transferred to the conducting band. A positive hole is created in the valence band. Therefore, the holes generated in the TiO_2 valence band can oxidize pollutants such as the dye, causing them to break down. Excited electrons can react with present species, such as oxygen and the H2O molecules, which are the sources of hydroxyl radicals ($OH^{\cdot}$) and superoxides ($O_2^{\cdot}$). Photogenerated positive holes, excited electrons, and reactive radicals can degrade the available organic species (e.g., dyes) by photo-oxidation and photo-reduction reactions (Nguyen and Kim 2022; Tang et al. 2014).

The function of silver metal caused by the electric field in the space-charge layer facilitates the transfer of excited electrons at the interface between Ag and TiO_2. Moreover, the combination of Ag_3PO_4 and TiO_2 promotes the effective separation of electrons and holes, leading to an enhancement in photocatalytic activity (Yao et al. 2012).

Few studies have been conducted on modifying titanium dioxide with silver and phosphate. By comparing the synthesis method in the present study to similar studies, it is evident that it demands the least, simplest, and cheapest materials. Other studies have used compounds such as tetrabutyl titanate (TBT) and titanium isopropoxide as the primary material for titanium dioxide. Commercial P25 powder was employed in this study. Furthermore, the approach employed in the synthesis is simpler and quicker than other synthesis methods. The process used is thermal precipitation and does not require processes such as sol–gel or photodeposition (Peng et al. 2019; Teng et al. 2013; Zhang et al. 2019). According to the study findings, the implemented modification has significantly lowered the band gap energy. Moreover, the performance of this compound is not significantly affected by the pH of the environment.

Considering the current constraints, exploring different calcination temperatures was not undertaken. Other temperatures may contribute to an increase in photocatalytic

efficiency. Furthermore, this study focused exclusively on silver and phosphate without exploring the potential effects of alternative metallic (Iron, copper, etc.) or non-metallic (Carbon, nitrogen, etc.) dopants. Investigating diverse dopants could provide valuable insights into the modulation of photocatalytic properties. Applying photocatalysts to various surfaces including, fabric, glass, or mineral substrates, can enhance its performance efficiency. However, it is paramount to note that in this study, the investigation was limited to the efficiency of the photocatalyst in powder form.

Conclusion

Characterization tests verified the heterostructure particles. Decorating TiO_2 with silver and phosphate ions extends the particles' light absorption into the visible spectrum by reducing the band gap to 1.94 eV. The coexistence of these two metallic and nonmetallic elements amplifies the density of photocurrent density and enhances the effective dissociation of electron–hole pairs formed during photo-induced activity.

The findings indicate that the removal efficiency of MB is not much affected by pH. Hence, it can be employed across a wide pH range to eliminate pollutants. The optimal particles performance was achieved with an initial concentration of 50 ppm using 3 g/l of photocatalyst over 45 min. Moreover, the efficiency of the removal of MB under sunlight illumination revealed a notably higher degree of efficacy than its removal under xenon visible light irradiation.

The findings from comparing the efficiency of modified particles with pure TiO_2 proved the excellent photocatalytic properties of Ag/Ag_3PO_4@ TiO_2 under visible light illumination. In optimal conditions, pure titanium dioxide exhibits approximately 50% less removal efficiency under ultraviolet radiation than Ag/Ag_3PO_4@ TiO_2 under visible radiation.

Accordingly, this composite can be a promising treatment method to recover various organic pollutants from water and wastewater supplies. It does not require any additional source of energy. It can consume solar light as activation energy at ambient conditions (temperature and pressure).

Acknowledgements This research was extracted from a thesis that Shiraz University of Medical Sciences supported. This plan has been approved by the Shiraz university of medical sciences ethics committee under code IR.SUMS.SCHEANUT.REC.1401.048.

Author Contributions All authors contributed to the study conception and design. Experimental conduction and writing original draft were performed by ZM. Project was administrated by MH. MD and MS guided experimental phase and analyzed data, respectively. The methodology was directed by AA and SJ. The manuscript was revised by MT. The study was conceptualized by AA as a supervisor and corresponding author.

Funding This work was supported by Shiraz University of Medical Sciences (Grant Numbers 25636). Abooalfazl Azhdarpoor has received research support from Shiraz University of Medical Sciences.

Data availability Data will be made available on request.

Declarations

Conflict of interest The authors declare no conflict of interest in terms of financial or personal nature for the publication of this article.

Ethical approval This declaration is not applicable.

References

Abukhadra MR, Shaban M et al (2018) Enhanced photocatalytic removal of Safranin-T dye under sunlight within minute time intervals using heulandite/polyaniline@ nickel oxide composite as a novel photocatalyst. Ecotoxicol Environ Saf 162:261–271. https://doi.org/10.1016/j.ecoenv.2018.06.081

Ahmad Barudin NH, Sreekantan S et al (2013) Antibacterial activity of Ag-TiO_2 nanoparticles with various silver contents. Mater Sci Forum 756:238–245

Alamu GA, Adedokun O et al (2021) Plasmonic enhancement of visible light absorption in Ag-TiO_2 based dye-sensitized solar cells. Chem Phys Impact 3:100037. https://doi.org/10.1016/j.chphi.2021.100037

Alkaim A, Aljeboree A et al (2014) Effect of pH on adsorption and photocatalytic degradation efficiency of different catalysts on removal of methylene blue. Asian J Chem 26(24):8445. https://doi.org/10.14233/ajchem.2014.17908

Alkaykh S, Mbarek A et al (2020) Photocatalytic degradation of methylene blue dye in aqueous solution by $MnTiO_3$ nanoparticles under sunlight irradiation. Heliyon 6(4):e03663. https://doi.org/10.1016/j.heliyon.2020.e03663

Alver E, Metin AÜ et al (2020) Methylene blue adsorption on magnetic alginate/rice husk bio-composite. Int J Biol Macromol 154:104–113. https://doi.org/10.1016/j.ijbiomac.2020.02.330

Anantha MS, Olivera S et al (2020) Comparison of the photocatalytic, adsorption and electrochemical methods for the removal of cationic dyes from aqueous solutions. Environ Technol Innov 17:100612. https://doi.org/10.1016/j.eti.2020.100612

Asenjo NG, Santamaria R et al (2013) Correct use of the Langmuir-Hinshelwood equation for proving the absence of a synergy effect in the photocatalytic degradation of phenol on a suspended mixture of titania and activated carbon. Carbon 55:62–69. https://doi.org/10.1016/j.carbon.2012.12.010

Chanu LA, Singh WJ et al (2019) Effect of operational parameters on the photocatalytic degradation of Methylene blue dye solution using manganese doped ZnO nanoparticles. Results in Phys 12:1230–1237. https://doi.org/10.1016/j.rinp.2018.12.089

Cushing SK, Li J et al (2012) Photocatalytic activity enhanced by plasmonic resonant energy transfer from metal to semiconductor. J Am Chem Soc 134(36):15033–15041. https://doi.org/10.1021/ja305603t

Del Angel R, Durán-Álvarez JC et al (2018) TiO_2-low band gap semiconductor heterostructures for water treatment using sunlight-driven photocatalysis. Titanium Dioxide: Mater Sustain Environ 305:70290. https://doi.org/10.5772/intechopen.70290

Dette C, Pérez-Osorio MA et al (2014) TiO_2 anatase with a bandgap in the visible region. Nano Lett 14(11):6533–6538. https://doi.org/10.1021/nl503131s

Dewidar H, Nosier S et al (2018) Photocatalytic degradation of phenol solution using Zinc Oxide/UV. J Chem Health Saf 25(1):2–11

Ding Y, Wu Y et al (2019) Colorful TiO_2-x microspheres cooperating with titanium Schiff base complex for efficient visible light photocatalysts. Catal Today 335:550–556. https://doi.org/10.1016/j.cattod.2019.03.004

Farooq MH, Aslam I et al (2019) Band gap engineering for improved photocatalytic performance of CuS/TiO_2 composites under solar light irradiation. Bull Chem Soc Ethiop 33(3):561–571. https://doi.org/10.4314/bcse.v33i3.16

Gan L, Xu L et al (2016) Preparation of core-shell structured $CoFe_2O_4$ incorporated Ag_3PO_4 nanocomposites for photocatalytic degradation of organic dyes. Mater Des 109:354–360. https://doi.org/10.1016/j.matdes.2016.07.043

Hamrouni A, Azzouzi H et al (2020) Enhanced solar light photocatalytic activity of ag doped TiO_2–Ag_3PO_4 composites. Nanomaterials 10(4):795. https://doi.org/10.3390/nano10040795

Hu M, Zhu P et al (2021) Construction of Ag_3PO_4/TiO_2/C with pn heterojunction using Shiff base-Ti complex as precursor: preparation, performance and mechanism. Powder Technol 393:597–609. https://doi.org/10.1016/j.powtec.2021.08.011

Jain R, Shrivastava M (2008) Photocatalytic removal of hazardous dye cyanosine from industrial waste using titanium dioxide. J Hazard Mater 152(1):216–220. https://doi.org/10.1016/j.jhazmat.2007.06.119

Karanasios N, Georgieva J et al (2015) Photoelectrocatalytic oxidation of organics under visible light illumination: a short review. Curr Org Chem 19(6):512–520. https://doi.org/10.2174/1385272819666150115000247

Khan I, Saeed K et al (2022) Review on methylene blue: its properties, uses, toxicity and photodegradation. Water 14(2):242. https://doi.org/10.3390/w14020242

Khezami L, Taha KK et al (2016) Adsorption and photocatalytic degradation of malachite green by vanadium doped zinc oxide nanoparticles. Water Sci Technol 73(4):881–889

Li Y, Sun S et al (2008) Kinetic study and model of the photocatalytic degradation of rhodamine B (RhB) by a TiO_2-coated activated carbon catalyst: effects of initial RhB content, light intensity and TiO_2 content in the catalyst. Chem Eng J 142(2):147–155. https://doi.org/10.1016/j.cej.2008.01.009

Lin X, Li M et al (2015) Enhancement of the catalytic activity of ordered mesoporous TiO_2 by using carbon fiber support and appropriate evaluation of synergy between surface adsorption and photocatalysis by Langmuir–Hinshelwood (L–H) integration equation. RSC Adv 5(127):105227–105238. https://doi.org/10.1039/C5RA21083F

Liu J, Weng M et al (2019) High-throughput HSE study on the doping effect in anatase $TiO_{(2)}$. Phys Chem Chem Phys 22(1):39–53. https://doi.org/10.1039/c9cp04591k

Liu H, Li D et al (2019) Fabrication and characterization of Ag_3PO_4/TiO_2 heterostructure with improved visible-light photocatalytic activity for the degradation of methyl orange and sterilization of E. coli. Mater Technol 34(4):192–203

Mosavi SA, Ghadi A et al (2021) Photocatalytic removal of Methylene Blue using Ag@CdSe/Zeoilte nanocomposite under visible light irradiation by response surface methodology. Mater Chem Phys 267:124696. https://doi.org/10.1016/j.matchemphys.2021.124696

Moztahida M, Lee DS (2020) Photocatalytic degradation of methylene blue with P25/graphene/polyacrylamide hydrogels: optimization using response surface methodology. J Hazard Mater 400:123314. https://doi.org/10.1016/j.jhazmat.2020.123314

Nagaraj G, Irudayaraj A et al (2019) Tuning the optical band Gap of pure TiO_2 via photon induced method. Optik 179:889–894. https://doi.org/10.1016/j.ijleo.2018.11.009

Nguyen NTA, Kim H (2022) Ag_3PO_4-deposited TiO_2@ Ti_3C_2 petals for highly efficient photodecomposition of various organic dyes under solar light. Nanomaterials 12(14):2464. https://doi.org/10.3390/nano12142464

Nyankson E, Efavi JK et al (2021) Synthesis of TiO $_2$–Ag_3PO_4 photocatalyst material with high adsorption capacity and photocatalytic activity: application in the removal of dyes and pesticides. RSC Adv 11(28):17032–17045. https://doi.org/10.1039/d1ra02128a

Otari SV, Yadav HM (2019) Photocatalytic active silver phosphate for photoremediation of organic pollutants. Photocatal Funct Mater Environ Remed 23:163–189. https://doi.org/10.1002/9781119529941.ch5

Pandey A, Kalal S et al (2015) Synthesis, characterization and application of naïve and nano-sized titanium dioxide as a photocatalyst for degradation of methylene blue. J Saudi Chem Soc 19(5):528–536. https://doi.org/10.1016/j.jscs.2015.05.013

Peng X, Zhang Y et al (2019) Fabrication of a novel high photocatalytic Ag/Ag_3PO_4/P25 (TiO_2) heterojunction catalyst for reducing electron-hole pair recombination and improving photo-corrosion. Mater Res Express 6(6):065515. https://doi.org/10.1088/2053-1591/ab0b88

Peng Y, Jiao A, et al. (2017). Abstract Submitted for the MAR17 meeting of the american physical society theoretical study on the possibility of S doping in anatase TiO_2

Rawal SB, Sung SD et al (2012) Novel Ag_3PO_4/TiO_2 composites for efficient decomposition of gaseous 2-propanol under visible-light irradiation. Catal Commun 17:131–135. https://doi.org/10.1016/j.catcom.2011.10.034

Rupa AV, Manikandan D et al (2007) Effect of deposition of Ag on TiO_2 nanoparticles on the photodegradation of Reactive Yellow-17. J Hazard Mater 147(3):906–913. https://doi.org/10.1016/j.jhazmat.2007.01.107

Salehi M, Hashemipour H et al (2012) Experimental study of influencing factors and kinetics in catalytic removal of methylene blue with TiO_2 nanopowder. Am J Environ Eng 2(1):1–7. https://doi.org/10.5923/j.ajee.20120201.01

Samal A, Baral A et al (2018) Silver phosphate based photocatalysis: a brief review from fundamentals to applications. Photocatal Nanomater Environ Appl 27:276–315

Schneider J, Matsuoka M et al (2014) Understanding TiO_2 photocatalysis: mechanisms and materials. Chem Rev 114(19):9919–9986. https://doi.org/10.1021/cr5001892

Singh J, Tripathi N et al (2019) Synthesis of Ag–TiO_2 hybrid nanoparticles with enhanced photocatalytic activity by a facile wet chemical method. Nano-Structures and Nano-Objects 18:100266. https://doi.org/10.1016/j.nanoso.2019.100266

Song Z, He Y (2017) Hydrothermal Synthesis of heterostructured Ag_3PO_4/TiO_2 photocatalyst with enhanced photocatalytic activity and stability under visible light. J Nanomater Biostruct 12(1):151–158

Sun X, Wang C et al (2020) Application of photocatalytic materials in sensors. Adv Mater Technol 5(5):1900993. https://doi.org/10.1002/admt.201900993

Tang C, Liu E et al (2014) Heterostructured Ag_3PO_4/TiO_2 nano-sheet film with high efficiency for photodegradation of methylene blue. Ceram Int 40(10):15447–15453. https://doi.org/10.1016/j.ceramint.2014.06.116

Teng W, Li X et al (2013) Fabrication of $Ag/Ag_3PO_4/TiO_2$ heterostructure photoelectrodes for efficient decomposition of 2-chlorophenol under visible light irradiation. J Mater Chem A 1(32):9060–9068. https://doi.org/10.1039/C3TA11254C

Wang J-L, Cheng F et al (2014) Structure and properties of urea-plasticized starch films with different urea contents. Carbohyd Polym 101:1109–1115. https://doi.org/10.1016/j.carbpol.2013.10.050

Xu C, Rangaiah G et al (2014) Photocatalytic degradation of methylene blue by titanium dioxide: experimental and modeling study. Ind Eng Chem Res 53(38):14641–14649. https://doi.org/10.1021/ie502367x

Xu Y, Liu X et al (2021) Ag_3PO_4 decorated black urchin-like defective TiO_2 for rapid and long-term bacteria-killing under visible light. Bioactive Mater 6(6):1575–1587. https://doi.org/10.1016/j.bioactmat.2020.11.013

Yang X, Fu H et al (2013) Hybrid Ag@ TiO_2 core–shell nanostructures with highly enhanced photocatalytic performance. Nanotechnology 24(41):415601. https://doi.org/10.1088/0957-4484/24/41/415601

Yao W, Zhang B et al (2012) Synthesis and characterization of high efficiency and stable Ag_3PO_4/TiO_2 visible light photocatalyst for the degradation of methylene blue and rhodamine B solutions. J Mater Chem 22(9):4050–4055. https://doi.org/10.1039/C2JM14410G

Zhang L, Yu D et al (2019) Fabrication of Ag_3 PO_4/TiO_2 composite and its photodegradation of formaldehyde under solar radiation. Catal Lett 149:882–890. https://doi.org/10.1007/s10562-019-02654-5

Zhang D, Lv S et al (2020) A study on the photocatalytic degradation performance of a [$KNbO_3$] 09-[BaNi 0.5 Nb 0.5 O_3− δ] 0.1 perovskite. RSC Adv 10(3):1275–1280. https://doi.org/10.1039/C9RA07310H

Zhou M, Li J et al (2015) Transfer charge and energy of Ag@ CdSe QDs-rGO core–shell plasmonic photocatalyst for enhanced visible light photocatalytic activity. ACS Appl Mater Interfaces 7(51):28231–28243. https://doi.org/10.1021/acsami.5b06997